

Optical Response of Large Lithium Clusters: Evolution toward the Bulk

C. Bréchnac, Ph. Cahuzac, J. Leygnier, and A. Sarfati

*Centre National de la Recherche Scientifique, Laboratoire Aimé Cotton, Bâtiment 505, Campus d'Orsay,
91405 Orsay CEDEX, France*

(Received 14 December 1992)

Multistep photon absorption has been used to measure the collective excitation of free lithium clusters having up to 1500 atoms. The blueshift of the Mie resonance energy, as cluster size increases, probes the surface effects. Its absolute value is consistent with the dielectric constants of the bulk down to a 100 atom cluster. The comparison with calculations in random-phase approximation in the local approximation demonstrates that the jellium model is no longer valid for lithium clusters.

PACS numbers: 78.20.Dj, 61.46.+w

The optical response of small metal particles as a function of size offers the possibility to follow the development of collective effects in metallic systems. Of these, alkali clusters, and in particular sodium and potassium, are regarded as a prototype of simple metallic particles. Their dipole absorption spectra are consistent with the optical excitation predicted by the classical Mie theory treatment of collective dipole oscillation in spherical or ellipsoidal distorted metallic droplets [1-4]. A more elaborate approach was obtained from time-dependent density-functional-theory calculations to quantitatively interpret the experimental data on sodium and potassium clusters having less than 40 atoms [5]. However, it was of fundamental interest to explore large cluster sizes to bridge the gap between the free small particles and the bulk in order to know to what extent the macroscopic dielectric function describes the optical response of metallic clusters.

We have developed recently an experimental procedure for extending optical absorption measurements [6] to large masses, i.e., a few thousand atoms. For large potassium clusters we have shown that the experimental value of the resonance energy evolves toward the infinite limit $\hbar\omega_M$ deduced either from the experimental volume plasmon energy $\hbar\omega_p$ [7] or from the surface plasmon energy $\hbar\omega_s$ [8]: $\hbar\omega_p \approx \hbar\omega_M\sqrt{3} \approx \hbar\omega_s\sqrt{2}$. Those values are close to the free-electron values. The small difference, less than 5%, which still remains between experimental values and free-electron values is greatly reduced when core polarization and effective mass are included [7,9].

Lithium metal differs from the other alkali metals. The measured volume plasmon energy is greatly shifted down from the free-electron value and its linewidth is very broad as compared to other alkali metals [10]. The deviation of the experimental plasmon-peak position from the free-electron value was mainly interpreted in terms of optical effective mass and is due to intraband transitions as pointed out by Paasch [11]. The volume plasmon linewidth in lithium was interpreted as a plasmon decay via interband transitions [10,12]. So the question arises as to whether such a deviation still exists for clusters. The measurement of the plasmon resonance of lithium

clusters is a real challenge to know to what extent the dielectric constants of the bulk are pertinent parameters to interpret the collective excitation of lithium clusters. If so, the microscopic calculation of the dynamic response of the electrons should interpret both cluster and bulk measurements.

In this Letter we report on the optical response of mass selected free lithium clusters Li_n^+ in the size range of 100 to 1500 atoms. Our results provide evidence of a broad surface plasmon resonance. The plasmon resonance energy is blueshifted as cluster size increases. The use of the measurements of the dielectric function $\epsilon(\omega)$ [13,14] in the determination of the Mie frequency is found to yield excellent extrapolation of the experimental cluster values when the cluster radius goes to infinity. The linewidth and resonance energy behavior are discussed and a comparison is done with the predictions of the random-phase approximation (RPA) in the local density approximation (LDA).

The experiment combines photon-interaction and mass spectroscopy [6]. Lithium clusters are formed by gas aggregation techniques which generate a neutral cluster distribution centered around 900 atom clusters [15]. The distribution is photoionized by a pulsed UV laser with photon energy $h\nu = 3.67$ eV. The accelerated cluster ion bunches first enter a field-free tube where they spatially resolve into separated ion packets within a mass resolution better than 200. After size selection a given cluster ion bunch enters a decelerating-accelerating region where it interacts with a second pulsed laser. We used a set of photon energies corresponding to Raman-shifted Nd-doped yttrium-aluminum-garnet laser frequencies. The photon energy lies in the region subtended by surface plasmon absorption, i.e., 1.8 to 4.7 eV. The ion products from photointeraction are mass analyzed by a second time-of-flight spectrometer.

It is well known that for metal clusters the electronic excitation, resulting from a photon absorption, whose energy is lower than the ionization potential, relaxes very rapidly among the numerous vibrational modes, providing heating of the cluster. As we have already shown [6], for large cluster sizes $n > 100$ several photons must be ab-

sorbed before the first evaporation can be observed. For measuring the absorption cross section of Li_n^+ we used the procedure based on multistep photon absorption followed by evaporation. The multistep photon absorption leads to a Poisson distribution for the fragments, the maximum of which gives the absorption cross section [6]. At a photon energy above ionization potential a new channel opens, making possible ionization threshold measurements, W_n^+ , as well as the absorption cross section measurements for Li_n^{++} .

Figure 1 shows the absorption cross section for Li_{139}^+ , Li_{270}^+ , Li_{820}^+ , and Li_{1500}^+ versus the photon energy. The errors bars result from the precision of determining the cross section from the fragment distribution. Experimental data for each cluster are fitted with a Mie-type resonance curve:

$$\sigma_n(h\nu) = \sigma_n^{\max} \frac{[h\nu\Gamma]^2}{[(h\nu)^2 - (h\nu_0)^2]^2 + [h\nu\Gamma]^2}, \quad (1)$$

where $h\nu_0$ is the resonance energy, Γ the width of the resonance, and σ_n^{\max} the absorption cross section at $h\nu_0$. The three fitting parameters $h\nu_0$, Γ , and σ_n^{\max} are given in Table I for the studied clusters. From Table I we observe the resonance energy shift toward the blue as n increases. The absorption cross section is roughly proportional to the number of atoms, which is also the number of valence electrons. The resonance width is large as compared to other alkalis [6,16] and to Li_8 [17]. The correction due to thermal expansion as explained in Ref. [6] is negligible in this case.

Contrary to other alkali clusters, ionization of Li_n^+ takes place in the energy range subtended by the Mie resonance. The lowest photon energy for which Li_n^{++} can be detected brackets the ionization threshold. It is interesting to compare our experimental values with the classical electrostatic model. From this model the energy which is necessary to remove an electron from an isolated uniform conduction sphere of radius R having Z elementary charges e [18] is

$$W_n^{z+} = W_\infty + (z + \frac{3}{8})e^2/R, \quad (2)$$

where W_∞ is the bulk work function. The equivalent sphere radius R of a metal cluster having n atoms is $r_s n^{1/3}$, where r_s is an electron density parameter [19]. With such a model the ionization threshold of Li_n^+ is

TABLE I. Resonance energy $h\nu_0$, resonance width Γ , and absorption cross section at $h\nu_0$, deduced from experimental data for several cluster sizes. The absolute cross section is given with 25% precision.

| | $h\nu_0$ (eV) | Γ (eV) | σ_n^{\max} (\AA^2) |
|----------------------|------------------|------------------|---|
| Li_{139}^+ | 2.92 ± 0.05 | 0.9 ± 0.1 | 62 |
| Li_{270}^+ | 3.06 ± 0.05 | 1.15 ± 0.1 | 120 |
| Li_{440}^+ | 3.17 ± 0.05 | 1.32 ± 0.1 | 280 |
| Li_{820}^+ | 3.21 ± 0.05 | 1.10 ± 0.1 | 440 |
| Li_{1500}^+ | 3.25 ± 0.05 | 1.15 ± 0.1 | 830 |

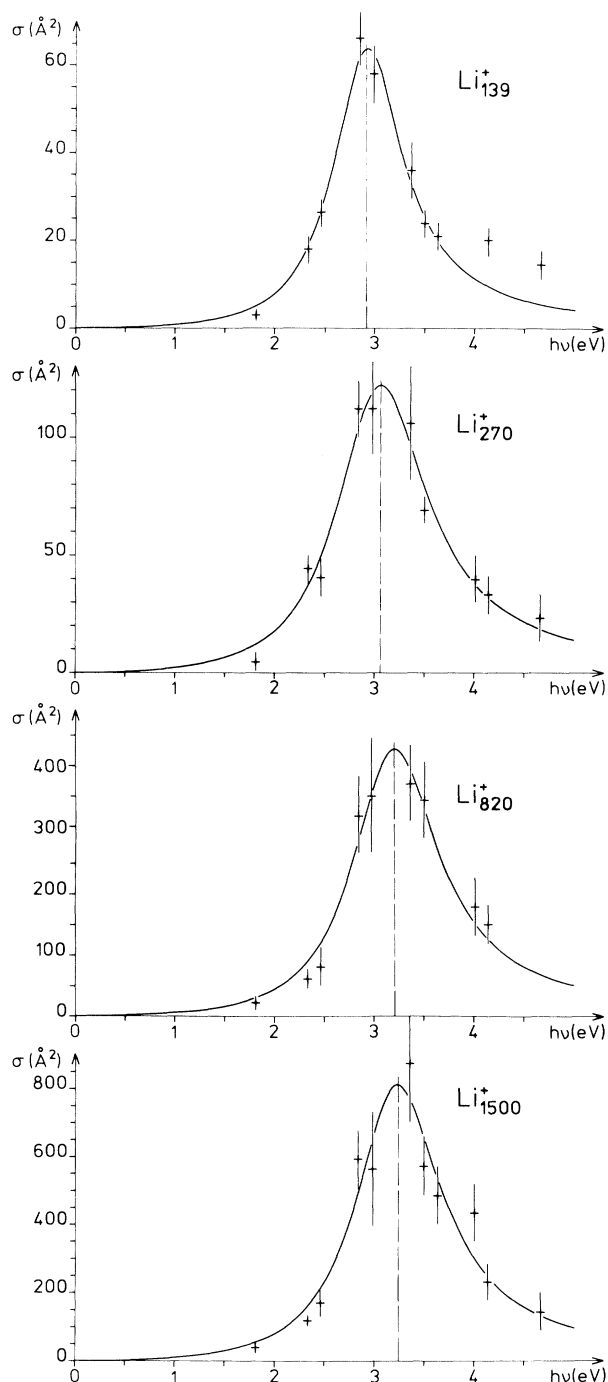


FIG. 1. Photoabsorption cross section profiles for large lithium cluster ions Li_n^+ as a function of photon energy. The parent masses are distributed around the mean mass through the resolution of the selection (few masses).

$$W_n^+ = W_\infty + \frac{11}{8} \frac{e^2}{r_s} n^{-1/3}. \quad (3)$$

In Fig. 2 are plotted the measured ionization potentials on an $n^{-1/3}$ scale. These values follow a linear behavior. The straight-line fit to the experimental data yields a value of $W_\infty = 2.55$ eV close to the polycrystalline work function [20] and a value of $r_s = 1.69$ Å in good agreement with the Wigner Seitz radius of bulk lithium, i.e., 1.72 Å. This indicates that r_s is a good parameter for describing electron density of both bulk and clusters.

In Fig. 2 are also plotted the measured peak resonance positions as a function of $n^{-1/3}$. Our measurements from $n = 129$ to $n = 1500$ fall on a straight line which can be easily extrapolated in the limit $1/R \rightarrow 0$ to $\hbar\omega_M = 3.55$ eV. The boundary conditions of a flat metallic surface imply that the surface plasma frequency is deduced from the dielectric function $\epsilon(\omega)$ in the vicinity $\epsilon(\omega) = -1$ [21]. For similar symmetrical reasons the boundary conditions of a spherical metallic surface imply that the surface plasmon frequency of a metallic sphere is deduced from the same dielectric function in the vicinity $\epsilon(\omega) = -2$. From the measurements of the macroscopic dielectric constant for lithium [13,14,22] the corresponding surface plasmon energy of a macroscopic metallic

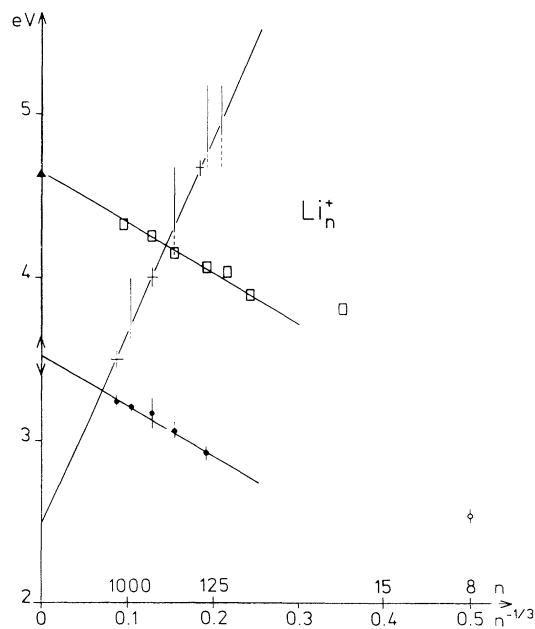


FIG. 2. Resonance energy and ionization potential (crosses) vs $n^{-1/3}$. The dots are the experimental resonance energies; the squares the RPA-LDA calculations. The open circle is the resonance energy of Li_8 from Ref. [17] in the $1/R \rightarrow 0$ limit. The RPA-LDA calculated values converge to the free-electron Mie energy $\hbar\omega_p/\sqrt{3} = 4.62$ eV (solid triangle). The experimental values converge to the energy deduced from $\epsilon(\omega) = -2$. Arrows represent the error bar of the experimental determination from Refs. [13,14,22].

sphere, also called the Mie frequency energy, is, in the long wavelength limit $R \ll \omega c$, $\hbar\omega_M = 3.55 \pm 0.1$ eV, in excellent agreement with our extrapolated value from cluster measurements. It has to be noted that for small cluster sizes such as Li_8 , from Ref. [17] the resonance peak position significantly deviates from the linear behavior.

It is interesting to compare the measured Mie resonance of Li_n^+ with the collective dipole excitation predicted by RPA-LDA calculations. The metallic cluster is treated as a homogeneous electron gas confined in a volume $V = \frac{4}{3}\pi nr_s^3$.

The electron correlation and exchange are approximated by a local function of density. The collective response of such a system only depends on r_s as a parameter. We have calculated the RPA-LDA response for different metallic spheres of different r_s with the program of Bertsch [23], which we have adapted for large masses. In Fig. 3 are given the results obtained for two different spheres having 440 electrons each, but different r_s values: $r_s = 1.70$ Å for Li and $r_s = 2.57$ Å for K, together with experimental results. It is clearly seen that the smaller the r_s value, the broader the oscillator strength distribution. This is consistent with the fact that among alkali metals, lithium, which has the smallest r_s value, exhibits the lowest correlation effects [7]. Although oscillator

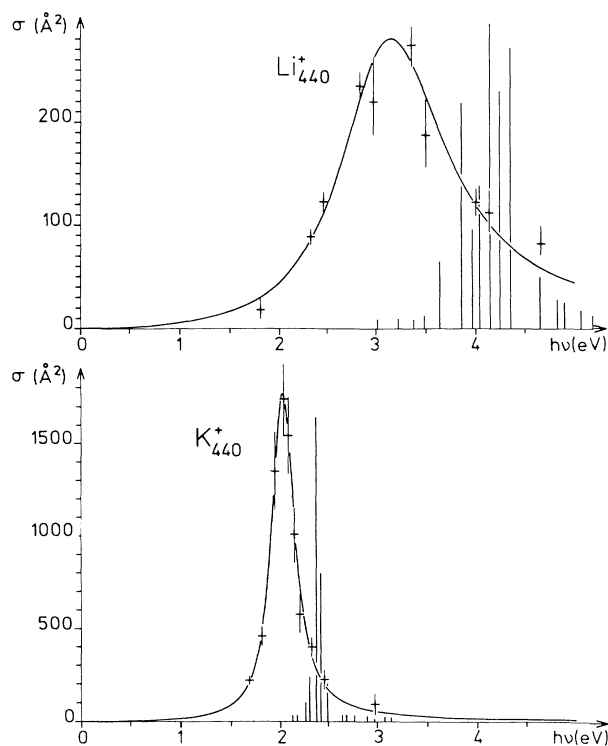


FIG. 3. Experimental photoabsorption cross section profile. Solid lines for Li_{440}^+ (present work) and K_{440}^+ (previous work [6]) together with RPA-LDA oscillator strength distribution (vertical bars).

strength distributions are less broad than the widths of the measured resonances, RPA-LDA calculations indicate that correlation effects should be partially responsible for the width of the cluster resonances.

Concerning the cluster resonance energy, the maximum of the calculated oscillator strength distribution is far from being in agreement with experimental data. In Fig. 2 is plotted the energy of the calculated RPA-LDA plasmon resonance for spherical lithium ($r_s = 1.7 \text{ \AA}$) as a function of cluster size. These calculated values are blueshifted as cluster size increases and converge, in the limit $1/R \rightarrow 0$, to the classical Mie value of a free-electron gas $\hbar\omega_{\text{Mie}} = \hbar\omega_p/\sqrt{3} = \hbar[e^2/mr_s^3]^{1/2} = 4.64 \text{ eV}$. Although the calculated RPA-LDA values are more than 1 eV above the experimental values it is interesting to notice that they each present a linear behavior versus $n^{-1/3}$ with equal slopes. Following Liebsch, who has shown that the momentum dispersion of the flat surface plasmon in the long wavelength regime and the variation of the Mie resonance of clusters at large R can both be expressed in terms of an effective local dielectric function [24], the slope of the straight line reflects the induced screening charge at the surface [22]. As for other alkalis the center of gravity of the charge fluctuation associated with the Mie resonance is located outside the volume of the cluster. Hence, the blueshift of the Mie resonance energy, as cluster size increases, probes the tail of the electron density outside the cluster volume, defined as the "spill out" effect [6,25]. The remarkable agreement between the slope corresponding to RPA-LDA calculations and that corresponding to experimental results indicates, as expected, that the valence electron gas in a lithium cluster is not perturbed by core electrons, contrary to the case of silver for which the proximity of the $4d$ electrons strongly influences the plasma resonance [24].

The discrepancy which exists between the experimental Mie peak position and the homogeneous RPA result was also observed for volume plasmon from electron energy-loss measurements [10]. For the bulk this difference was interpreted essentially by an effective mass [12]. In fact the effective mass contribution, which is also in pseudopotential theory the intraband contribution, depends mainly, in the Li case, on electron-ion-core interactions. The homogeneous RPA calculation which treats positive ionic cores as a uniform positive background is not sufficient to interpret the experimental data. In a first step, improvement should be made by introducing an Ashcroft empty core local potential which takes into account Coulomb electron-ion-core interactions [26].

In conclusion, our measurements on the optical response of lithium clusters show evidence that the macroscopic dielectric function is a pertinent parameter to interpret cluster data. In fact our results point out that such a macroscopic function is still present in clusters

containing 100 atoms, i.e., 10 \AA radius, for which *ab initio* microscopic calculations can be done beyond the jellium model. Moreover the linear behavior of the Mie resonance in the long wavelength limit versus the cluster radius corresponds to surface effects and can be related to surface plasmon dispersion.

We would like to thank A. Liebsch for suggesting the relation between excitation of small particles and momentum dispersion of flat surface plasmon, U. Landman for stimulating discussions on the dielectric constant, and C. Guet for sending us his results prior to publication.

-
- [1] G. Mie, *Ann. Phys. (Leipzig)* **25**, 377 (1908).
 - [2] R. Gans, *Ann. Phys. (Leipzig)* **47**, 270 (1913).
 - [3] D. Skillman and C. R. Berry, *J. Chem. Phys.* **48**, 3297 (1968).
 - [4] W. de Heer, K. Selby, V. Kresin, J. Masui, M. Vollmer, A. Châtelain, and W. Knight, *Phys. Rev. Lett.* **59**, 1805 (1987).
 - [5] W. Ekardt and Z. Penzar, *Phys. Rev. B* **43**, 1322 (1991).
 - [6] C. Bréchnignac, Ph. Cahuzac, N. Kebaili, J. Leygnier, and A. Sarfati, *Phys. Rev. Lett.* **68**, 3916 (1992).
 - [7] A. V. Felde, J. Sprösser-Prou, and J. Fink, *Phys. Rev. B* **40**, 10181 (1989).
 - [8] K. Ding Tsuei, E. W. Plummer, and P. J. Feibelman, *Phys. Rev. Lett.* **63**, 2256 (1989).
 - [9] K. Sturm, *Solid State Commun.* **48**, 29 (1983).
 - [10] P. C. Gibbons, S. E. Schnatterly, J. J. Ritsko, and J. R. Fields, *Phys. Rev. B* **13**, 2451 (1976); **15**, 2420 (1977).
 - [11] G. Paasch, *Phys. Status Solidi* **38**, K123 (1970).
 - [12] K. Sturm, *Adv. Phys.* **31**, 1 (1982).
 - [13] J. N. Hodgson, in *Optical Properties and Electronic Structure of Metals and Alloys*, edited by F. Abeles (North-Holland, Amsterdam, 1966), p. 60.
 - [14] M. Rasigni and G. Rasigni, *J. Opt. Soc. Am.* **67**, 54 (1977).
 - [15] C. Bréchnignac, Ph. Cahuzac, F. Carlier, M. de Frutos, and J. Ph. Roux, *Phys. Rev. B* **47**, 2271 (1993).
 - [16] C. C. Wang, S. Pollack, and M. Kappes, *Chem. Phys. Lett.* **166**, 26 (1990).
 - [17] J. C. Blanc, V. Bonacic Koutecky, M. Broyer, J. Chevalyere, Ph. Dugourg, J. Koutecky, C. Scheuch, J. P. Wolf, and L. Wöste, *J. Chem. Phys.* **96**, 1793 (1992).
 - [18] L. D. Landau and E. Lifchitz, *Electrodynamics of Continuous Media* (MIR Editions, Moscow, 1969).
 - [19] N. W. Ashcroft and N. D. Mermin, *Solid State Physics* (Holt Saunders, Tokyo, 1976).
 - [20] H. B. Michaelson, *J. Appl. Phys.* **48**, 4729 (1977).
 - [21] P. Feibelman, *Phys. Rev. B* **40**, 2752 (1989).
 - [22] A. G. Mathewson and H. P. Myers, *Phys. Scr.* **4**, 291 (1971).
 - [23] G. Bertsch, *Comput Phys. Commun.* **60**, 247 (1990).
 - [24] A. Liebsch (to be published).
 - [25] E. Engel and J. Perdrew, *Phys. Rev. B* **43**, 1331 (1991).
 - [26] C. Guet (to be published).